Article

Tubular Configurations and Structure-Dependent Anisotropic Strains in GaS Multi-Walled Sub-Microtubes

Fang-Fang Xu, Junqing Hu, and Yoshio Bando

J. Am. Chem. Soc., **2005**, 127 (48), 16860-16865• DOI: 10.1021/ja053340z • Publication Date (Web): 28 October 2005

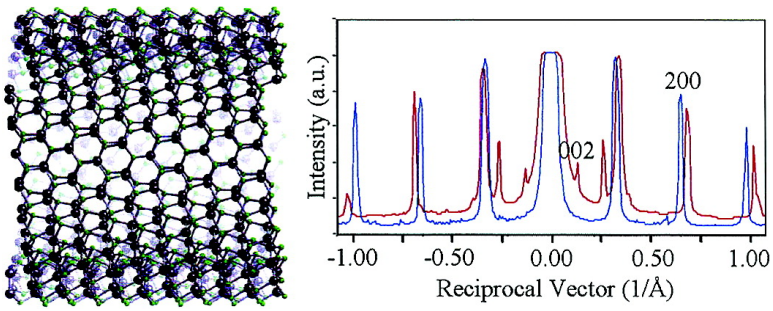

More About This Article

Additional resources and features associated with this article are available within the HTML version:

- Supporting Information
- Links to the 2 articles that cite this article, as of the time of this article download
- Access to high resolution figures
- Links to articles and content related to this article
- Copyright permission to reproduce figures and/or text from this article

View the Full Text HTML

J|A|C|S
ARTICLES
Published on Web 10/28/2005

Tubular Configurations and Structure-Dependent Anisotropic Strains in GaS Multi-Walled Sub-Microtubes

Fang-Fang Xu,*,† Junqing Hu,‡ and Yoshio Bando§

Contribution from the Shanghai Institute of Ceramics, Shanghai 200050, People's Republic of China, and International Center for Young Scientists (ICYS) and Advanced Materials Laboratory, National Institute for Materials Science, Tsukuba, Ibaraki 305-0044, Japan

Received May 22, 2005; E-mail: ffxu@mail.sic.ac.cn

Abstract: Bending strains and bonding structures of GaS multiwalled submicrotubes have been examined by transmission electron microscopy. Experimental observations reveal that the strain involved in building the GaS tubes is more complicated than the theoretical prediction and appears anisotropic and dependent on the tubular configurations. The armchair tube bears a larger lattice compression than the zigzag tube. The hexagonal GaS semiconducting compound degrades its crystal symmetry upon bending, leading to the anisotropy of the bonding structures. Curving of GaS sheets to form tubes is found to be dominated by the structures and electrostatic fields on the sheet surface, which eventually gives a well-controlled tubular structure showing preferred zigzag and close-to-zigzag configurations. Finally, interlayer packing structures of multiwalled tubes are examined.

Introduction

Following the pioneering work on carbon nanotubes[1] and applying the chemical analogy between graphite and two-dimensional (2-D) layered inorganic compounds, a growing number of tubular materials has been synthesized, which provides the opportunity to study the chemistry and physics of systems with reduced dimensionality. Besides the BN nanotube,[2] the critical isostructural derivative of the carbon nanotube, the first inorganic nanotubes were obtained by Tenne and co-workers, who successfully prepared metal−disulfide nanotubes $X-S_2$ (X = Mo, W).[3,4] To date, the observed inorganic compounds that curve include BN,[2] $NiCl_2$,[5] and a variety of metal−chalcogenides (e.g., VO_x,[6] WS_2,[3] MoS_2,[4] InS,[7] GaS,[8−10] and GaSe[9] etc). Bending a planar filament to form a tube requires more energy to overcome the high strain arising from the bond distortion. It has been derived that the strain energy, the energy difference between a tube and its parent planar structure, is proportional to the square of curvature ($\propto R^{-2}$).[11,12] Generally, the driving force to bend a filament is provided by the catalytic particles whose size, structure, and shape determine the configuration and diameter of the nanotubes growing on them.[13,14] However, some tubes can be generated in the absence of catalysts and were considered to initiate from topological defects such as five-membered rings at the tip.[15] Recently, the development of soft chemistry made some layered oxides form ultrathin 2-D sheets.[16,17] The high surface-to-volume ratio of nanosheets raises the system energy and makes them unstable. Therefore, nanosheets curve and roll to form tubes.[18] Nevertheless, the tubes formed by rolling the filaments usually have large diameters due to the weak driving force for curving.

Sulfides and selenides of III-group metals exhibit 2-D layered structures, bounded by van der Waals attractions. Recently, hexagonal InS, GaSe, and GaS tubes have been synthesized, which evidenced the theoretical prediction of stable tubular structures of these compounds.[19,20] By adopting the conventional nomenclature for the description of carbon nanotubes,[21] hexagonal GaS nanotubes, for example, can form both zigzag (n,0) and armchair (n,n) configurations. The density-functional tight-

† Shanghai Institute of Ceramics.
‡ ICYS, National Institute for Materials Science.
§ Advanced Materials Laboratory, National Institute of Materials Science.

(1) Iijima, S. *Nature* **1991**, *354*, 56.
(2) Chopra, N. G.; Luyren, R. J.; Cherry, K.; Crespi, V. H.; Cohen, M. L.; Louie, S. G.; Zettl, A. *Science* **1995**, *269*, 966.
(3) Tenne, R.; Margulis, L.; Genut, M.; Hodes, G. *Nature* **1992**, *360*, 444.
(4) Feldman, Y.; Wasserman, E.; Srolovitz, D. J.; Tenne, R. *Science* **1995**, *267*, 222.
(5) Hachohen, Y. R.; Grunbaum, E.; Tenne, R.; Sloan, J.; Hutchison, J. L. *Nature* **1998**, *395*, 336.
(6) Ajayan, P. M.; Stephan, O.; Redlich, Ph.; Colliex, C. *Nature* **1995**, *375*, 564.
(7) Hollingsworth, J. A.; Poojary, D. M.; Clearfield, A.; Buhro, W. E. *J. Am. Chem. Soc*. **2000**, *122*, 3562.
(8) Hu, P. A.; Liu, Y. Q.; Fu, L.; Cao, L. C.; Zhu, D. B. *Appl. Phys. A* **2005**, *80*, 1413.
(9) Gautam, U. K.; Vivekchand, S. R. C.; Govindaraj, A.; Kulkarni, G. U.; Selvi, N. R.; Rao, C. N. R. *J. Am. Chem. Soc*. **2005**, *127*, 3658.
(10) Hu, J. Q.; Bando, Y.; Zhan, J. H.; Liu, Z. W.; Golberg, D. *Appl. Phys. Lett.* **2005**, *87*, 153112.
(11) Tibbets, G. G. *J. Cryst. Growth* **1984**, *66*, 632.
(12) Robertson, D. H.; Brenner, D. W.; Mintmire, J. W. *Phys. Rev. B* **1992**, *45*, 12592.
(13) Iijima, S.; Ichihashi, T. *Nature* **1993**, *363*, 603.
(14) Bethune, D. S.; Kiang, C. H.; de Vries, M. S.; Gorman, G.; Savoy, R.; Vazquez, J.; Beyers, R. *Nature* **1993**, *363*, 605.
(15) Wakabayashi, T.; Achiba, Y. *Chem. Phys. Lett.* **1992**, *190*, 465.
(16) Treacy, M. M. J.; Rice, S. B.; Jacobson, A. J.; Lewandowski, J. T. *Chem. Mater*. **1990**, *2*, 279.
(17) Sasaki, T.; Watanabe, M.; Hashizume, H.; Yamada, H.; Nakazawa, H. *J. Am. Chem. Soc*. **1996**, *118*, 8329.
(18) Saupe, G. B.; Waraksa, C. C.; Kim, H. N.; Han, Y. J.; Kaschak, D. M.; Skinner, D. M.; Mallouk, T. E. *Chem. Mater*. **2000**, *12*, 1556.
(19) Côté, M.; Cohen, M. L.; Chadi, D. J. *Phys. Rev. B* **1998**, *58*, R4277.
(20) Köhler, T.; Frauenheim, T.; Hajnal, Z.; Seifert, G. *Phys. Rev. B* **2004**, *69*, 193403.
(21) Dresselhaus, M. S.; Dresselhaus, G.; Saito, R. *Phys. Rev. B* **1992**, *45*, 6234.

10.1021/ja053340z CCC: $30.25

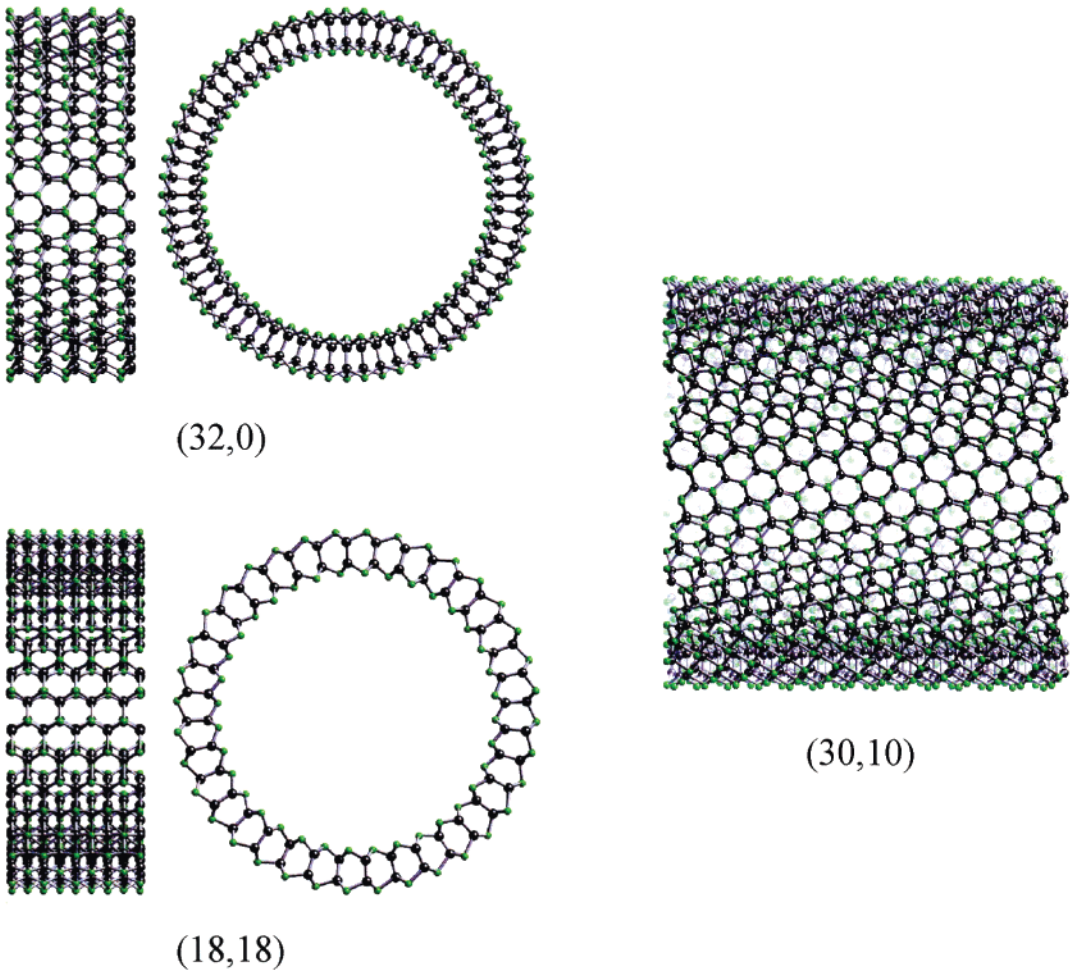

Figure 1. Structural models of (32,0) zigzag, (18,18) armchair, and (30,10) helical GaS nanotubes. Both normal (left) and parallel (right) views to the nanotube axis are presented for the zigzag and armchair configurations.

binding calculations suggest a stable hexagonal double-layered curved structure composed of S−Ga−Ga−S bonding chains arranged in six-membered Ga_3S_3 rings,[20] as shown in Figure 1. Therefore, it is considered that the diameter of the GaS nanotube cannot be smaller than 3.6 nm, otherwise it becomes unstable due to strong distortions of Ga−S bonds at inner and outer surfaces. The GaS single-walled nanotubes have a semiconducting direct gap irrespective of the helicity. The strain energy is a function of the mean diameter of the nanotube. Such anticipation of physical properties is based on a fully relaxed single-walled nanotubular structure.[20] However, it will be seen that the experimentally obtained GaS tubes in this work have multiwalled structures and show structural features far from the ideal ones that the theoretical calculation predicted. More complicated strains are involved in building the tubular morphology. In this paper, we describe a thorough investigation of structural strains in the GaS multiwalled submicrotubes by transmission electron microscopy (TEM). The experimental observation revealed that reduction in dimensionality for an inorganic layered compound resulted in degradation of crystal symmetry and anisotropy of bonding structures, which depends on the bending directions.

Experimental Procedures

Materials Preparation. GaS submicrotubes were synthesized via a simple high-temperature thermal reaction with the starting materials of Ga_2O_3, ZnS, and activated carbon powders. Decomposition of source materials was followed by thermal reactions between gallium and sulfur or gallium oxide and carbon sulfide at a high temperature and in a carrying flow of pure Ar. The obtained products include GaS sheets and submicrotubes. Details of synthesis will be reported elsewhere.[10]

Structural Analysis. Structures of GaS submicrotubes were examined by transmission electron microscopy. Electron diffraction patterns and high-resolution electron microscopy images were obtained on a JEM-2100F field-emission transmission electron microscope. Tubular configurations were derived from the mutual arrangement of reflections from both the hollow and the sidewall regions of the tubes. Structural strain was measured using the DigitalMicrograph (Gatan) software package by comparing diffraction patterns from both the sheets and the tubes, which were acquired with exactly the same TEM technical parameters and within an individual machine time.

Results and Discussion

Electron microscopy shows that the GaS tubes have lengths up to tens of micrometers. The diameters range in 200−900 nm with the wall thickness around one-third of the diameter (see Figure 2a). Electron diffractions show typical patterns of a bending geometry, which consists of reflections from both the side walls (cross-sections of filaments) and the inner regions (plane view of filaments). Because the GaS tubes have a very large size and thick walls, in-plane $\{hk0\}$ reflections become dots rather than arches as generally observed in fine carbon nanotubes.[22] Thus, this excludes the possible measurement errors

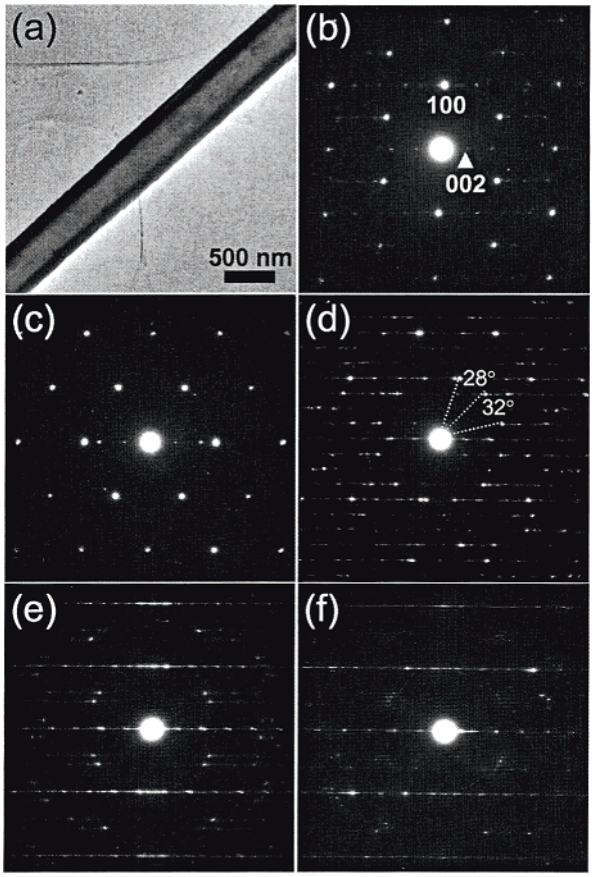

Figure 2. TEM micrograph of the GaS submicrotube (a) and electron diffraction patterns of the tubes showing (b) zigzag, (c) armchair, (d) large-angle monohelical, (e) small-angle monohelical, and (f) small-angle double-helical configurations. Panels e and f refer to the close-to-zigzag configurations.

arising from the contribution of reflections from otherwise oblique thin tubular shells, which may cause about 1−2% smaller lattice parameters than the real ones. The helicity of the tubes can be identified by the mutual arrangement of reflections from inner and wall regions. We acquired diffraction patterns from over 20 GaS tubes, which were not so thick as to allow the electron beams to transmit through the samples. The results demonstrate that almost all the GaS tubes display a zigzag (Figure 2b) or close-to-zigzag configuration (Figure 2e,f), while armchair (Figure 2c) and large-angle helical (Figure 2d) structures were observed each in one tube. The close-to-zigzag structure has a rotation (helical) angle of no more than 7° from the zigzag configuration, indicative of the tubular (n,m) configurations with the n/m ratio larger than 7. The diffraction pattern shown in Figure 2d represents the maximum rotation angle ever for a helical configuration (i.e., ∼14° to the armchair and ∼16° to the zigzag orientation). This configuration refers to the (3n,n) helical structure. The structural model of the (30,10) GaS nanotube is shown in Figure 1 as an example. Unlike multiwalled carbon nanotubes that usually show multiple helicity, the GaS tubes display monohelicity. Only two sets of a [001]-projected diffraction pattern (i.e., {hk0} reflections), each from the upper and bottom shells of a lying tube normal to the electron beam, are observed for the helical tubes. Double helicity was detected only in one tube as shown in Figure 2f. The helical angle exhibits 2.5 and 7° for the two tubular compartments, respectively. Low helical multiplicity implies high crystallinity along the radial direction of the GaS tubes. It seems that, at least, the helical GaS tube is more like a rolled tube rather than a seamless cylinder because the rolling of a sheet belt can guarantee the monohelicity.

Since the growth unit of a stable GaS tubular structure involves four atomic layers, large atomic displacement is expected at surface sulfur layers upon bending.[20] Although the present GaS tubes have diameters in submicrometer scales, larger lattice strains than expected were observed as evidenced by the measurement of lattice parameters on electron diffraction patterns. Under the same TEM technical conditions with the optimum objective lens current and within an individual machine time, we obtained diffraction patterns from both the GaS sheets and the GaS tubes, which coexisted in the present product. Anisotropic lattice strain was then observed in the GaS tubes. Meanwhile, the magnitude of strain depends on the tubular configuration. Figure 3 shows the profiles of reflections arrayed normal or parallel to the armchair and the zigzag tube axes along with those from the GaS sheets for comparison. The armchair tube exhibits the largest in-plane lattice compression by 4.3% (Figure 3a) in the direction perpendicular to the tube axis, while the lattice along the tube axis appears slightly expanded by 0.7% (Figure 3b). In contrast to the high anisotropy of lattice strain in the armchair tube, the zigzag tube (see Figure 3c,d) shows somewhat isotropic strains with the lattice compression by 1.8% across the tube axis and by 2.1% along the tube axis. The measurement of lattice parameters indicates that the magnitude of lattice compression is around 2% for all zigzag and close-to-zigzag tubes but that the strain differs slightly in the two directions. However, the large-angle helical (3n,n) GaS tube did not show any changes in the lattice parameters. Although the strain is absolutely dependent on the curvature of tubes (i.e., the diameters), the experimental observation of the present GaS submicrotubes does not show apparent dependence of strains on the diameters in the range of 200 to ∼900 nm. The diameters might be too large to be sensitive to the strain difference. It seems that the observed strain property is intrinsic to the layered structure of GaS. It is reasonable to consider that the in-plane lattice compression should undergo a simultaneous lattice expansion normal to the sheet plane. However, the measurement on the diffraction pattern does not show any detectable changes of the c-dimension in the GaS tubes. This implies an in-plane compressed unit cell in the GaS tubes with, anisotropically, decreases in Ga−S bond lengths along with the changes in bond angles, hence the degradation of crystal symmetry.

Different distorted structures observed in armchair and zigzag tubes suggest a structure-dependent strain in this bending compound. We then investigated the bonding structures of armchair and zigzag tubes bearing a certain identical strain. A compressive stress is applied normal to the zigzag (marked by filled arrows) and armchair (marked by blank arrows) tube axis as previewed in Figure 5. The stress was supposed to make the lattice shrink by 5% only along the stress direction while keeping the lattice parameters in the directions normal to it constant in a similar accordance to the experimental observation for the armchair tube. Curved GaS sheets in a tube no longer display a hexagonal symmetry but 1-D periodicity along the tube axis. Nevertheless, the zigzag and armchair tube shells can be

(22) Dresselhaus, M. S.; Dresselhaus, G.; Saito, R. *Carbon* **1995**, *33*, 883.

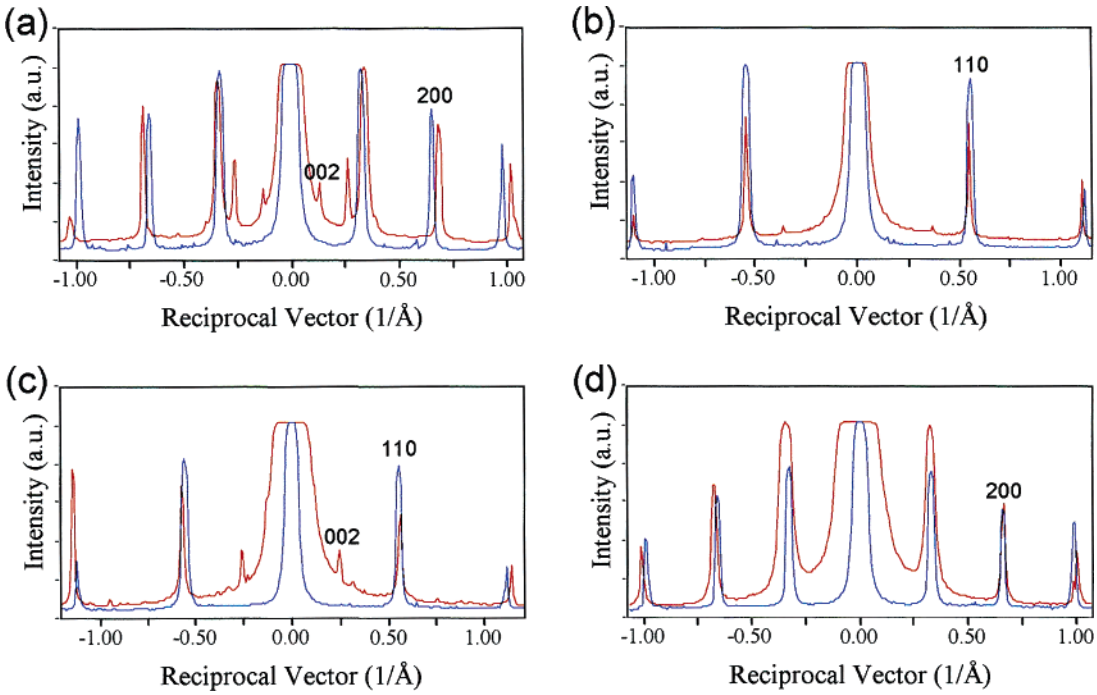

Figure 3. Anisotropic lattice strain in GaS tubes as revealed via measuring and comparing the lattice parameters of the GaS tubes (red lines) and GaS sheets (blue lines) obtained on the diffraction patterns. Both reflection profiles across an armchair tube (a) and a zigzag tube (c) and along the tube axis ((b) for armchair and (d) for zigzag tube) were presented. All the diffraction patterns were acquired using the same TEM technical parameters and within an individual machine time.

approximately regarded as different orthorhombic structures as framed by the dotted lines and dashed lines, respectively, in Figure 5. Under a sole compressive stress normal to the tube axis, the lattice shrinks while maintaining the orthorhombic symmetry to avoid an increase of the system energy arising from lowering the crystal symmetry. The orthorhombic lattice dimensions change only in the stress direction. Therefore, in the zigzag tube, the original bonds normal to the stress direction remain unchanged during the compression. Meanwhile, structural relaxation was performed via adjusting the atomic positions so as to retain as much as possible the symmetrical operations in the orthorhombic lattice (e.g., trying to show as uniform a bond length and angles as possible). This was carried out manually using the CrystalMaker software. The bond length and bond angles in the deformed structures can then be derived as listed in Table 1. Behind the same magnitude of lattice strain, bigger changes in bond length and bond angles were found in zigzag tubes along with a more severe degradation of crystal symmetry as evidenced by the variety of bond data. Therefore, the bonding structures tend to be more anisotropic in the zigzag configuration under such deformation processes. Actually, the observed strain mode in zigzag tubes applied a more isotropic fashion, trying to maintain the hexagonal symmetry to depress the increase of system energy arising from an otherwise inhomogeneous bond distortion. It seems that the armchair tube can withstand a larger lattice strain (not bond distortion) than the zigzag tube under identical stress, hence the bigger modification in the observed lattice parameters. The present observation is inconsistent with the theoretical prediction, which shows that the strain energy is solely dependent on the mean diameter of the tube irrespective of the tubular configurations.[20] Anisotropy and structure dependence of strains observed in the present GaS multiwalled submicrotubes indicate different structural relaxation kinetics

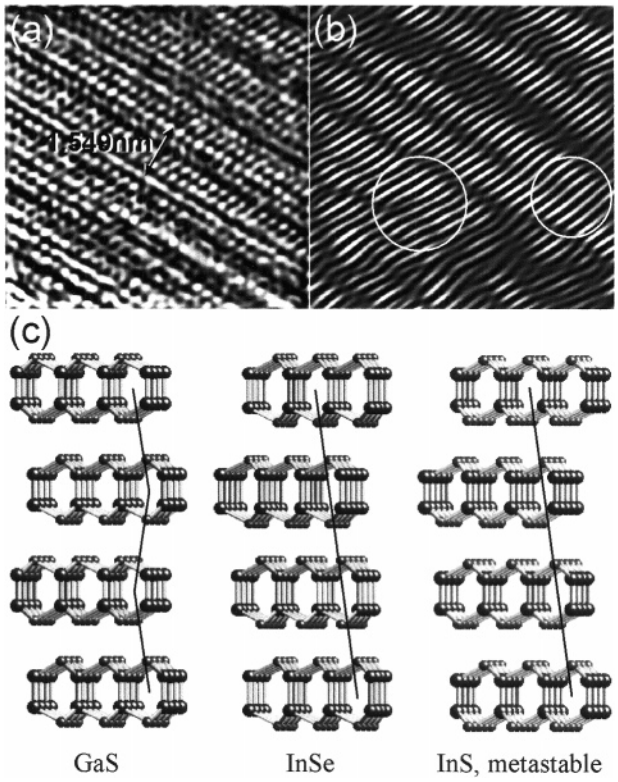

Figure 4. Metastable rhombohedral GaS phase as observed by high-resolution electron microscopy. (a) The lattice image from the wall region of a close-to-zigzag tube showing periodic layered structures. (b) The inverse fast-Fourier transformed micrograph calculated with the {0*kl*} reflections obtained from panel a, illustrating the typical ABC packing structures (circled regions) characteristic of the rhombohedral symmetry. (c) In-layer and packing structures of hexagonal GaS and rhombohedral InSe and InS structures.

Table 1. Bond Data of the GaS Crystal, Deformed Zigzag, and Deformed Armchair Structures

	Ga–S bond length (Å)	S–Ga–S bond angle (deg)	Ga–S–Ga bond angle (deg)	Ga–Ga–S bond angle (deg)
GaS crystal	2.353	99.326	99.326	118.337
deformed zigzag	2.353	99.605 (+0.28%)	99.605 (+0.28%)	119.255 (+0.78%)
	2.285 (−2.89%)	96.415 (−2.93%)	96.415 (−2.93%)	118.337
deformed armchair	2.317 (−1.53%)	101.397 (+2.09%)	97.343 (−2.00%)	118.807 (+0.40%)

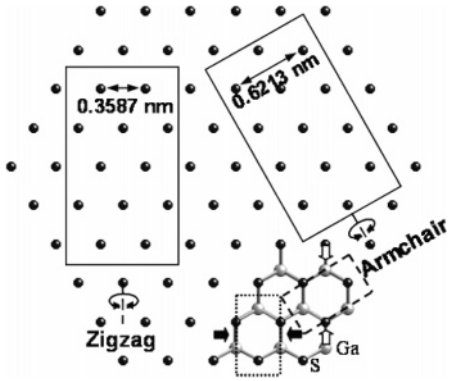

Figure 5. Structures of the surface sulfur layer in the hexagonal GaS layered compound. The strong electrostatic force between the nearest S atoms on the surface eventually leads to the formation of zigzag tubes upon rolling.

from conventional suggestions. Even bigger and more complicated structural distortion could be expected for GaS tubes with reduced diameters (e.g., nanotubes). It is noted that changes in lattice parameters and crystal symmetry in the GaS tubes surely affect their electronic structures. A reevaluation of physical properties of GaS tubes should be performed by taking into account the structural features observed herein. It seems that the 3-D network of GaS bending layers is less strong than the 2-D graphene sheet, hence the ease of lattice distortion upon bending. The lowest strain observed in the large-angle helical tube may imply its rolled nature rather than a seamless cylinder, where the strain is easily released via interlayer lattice displacement. In Table 1, the data listed in parentheses are changes in percentage with respect to the bond data of GaS crystal.

The bending of GaS sheets distorts the crystal structure, and structural defects have been found to form in almost every GaS tube. Electron diffractions in Figure 2 display streaks along the [00*l*] reciprocal vectors, indicative of a high density of stacking faults formed in the GaS tubes. The reflection streaks on a diffraction pattern indicate lattice displacements with certain lattice vectors rather than random displacements. High-resolution electron microscopy of GaS submicrotubes revealed a rhombohedral GaS phase intergrowing locally with the hexagonal lattice. Figure 4b shows the inverse fast-Fourier transformed micrograph from the original lattice image (Figure 4a) of the sidewall region calculated by using {0*kl*} reflections. It is noted in Figure 4c that the GaS hexagonal ($P6_3/mmc$) structure shows an inversion operation along with a 1/3[210] displacement between the two neighboring layers. When viewed along the [100] direction of a close-to-zigzag tube, the packing structure shows a typical ABAB packing pattern. However, the circled regions in Figure 4b illustrate the ABC... packing pattern typical of rhombohedral symmetry. Selenide[23,24] and sulfide[7] of indium have been reported to show different rhombohedral structures (Figure 4c). The InSe-type structure seems more reasonable for the GaS system because the double-layer packing unit shows the same configuration. But here, no inversion takes place for the neighboring layers, but only a lattice displacement is involved. Partial dislocations can be observed at the boundaries of different phases in Figure 4b. The GaS rhombohedral phase seems to be a metastable structure and involves only very fewer layers.

GaS tubes have been proven to form by natural curving of the GaS sheets rather than onto the catalytic particles.[10] A thin sheet is an unstable structure because of its high surface-to-volume ratio and high system energy. Curving of sheets can reduce the number of unsaturated dangling bonds on the surface and thus lower its system energy. The driving force to curve a nanosheet arises from the electrostatic forces on the surface.[18] The diameter of the formed tubes relies on the competition between the driving force and the strain energy in a curved structure. Although the previous analysis indicates that it is easier to bend a GaS sheet according to the armchair configuration, the experimental observation found a prevailing formation of zigzag tubes. Therefore, we investigated the structures and electrostatic field on the GaS sheet surface in an attempt to explain the formation mechanism of GaS tubes. The surface of GaS sheets is composed of unsaturated S atoms as shown in Figure 5. Each S atom has six nearest neighbors in 0.3587 nm and six second nearest neighbors in 0.6213 nm. The electrostatic force (Coulomb attraction) is inversely proportional to the interatomic distances. Therefore, the nearest neighbor S atoms show higher attraction forces and tend to be closer, leading to a final zigzag tubular configuration (Figure 5). This bending performance does not apply to the graphene sheets where all bonds are parallel to the lateral plane, hence high stiffness and bend modulus. However, the counterpart of high distortion in bending a four-atomic-layered shell unit in GaS system is its low bend modulus because no bonds are parallel to the sheet plane. The 3-D bonding structure is easy to relax along the bending tangential (see Figure 1) via reconstruction of all four atomic layers. Therefore, the as-obtained GaS tubes show a certain uniform helix dominated by the surface structure. However, the electrostatic forces are weak on the surface so that the GaS tubes synthesized by the present method are fairly large. Small GaS tubes shall be formed via another mechanism (e.g., with the aid of catalytic particles), but in that case, the helicity of the tube can hardly be controllable.

Conclusion

Anisotropic and structure-dependent strains were observed in GaS submicrotubes, showing reduced lattice parameters and degradation of crystal symmetry. Analysis of deformed bonding structure suggests that the armchair tubes can withstand higher structural strains than the zigzag tubes. However, the present GaS tubes display the preference to zigzag and close-to-zigzag tubular configurations. This structural feature has been explained

(23) Likforman, A.; Carré, D.; Etienne, J.; Bachet, B. *Acta Crystallogr., Sect. B* **1975**, *31*, 1252.
(24) Rigoult, J.; Rimsky, A.; Kuhn, A. *Acta Crystallogr., Sect. B* **1980**, *36*, 916.

by considering the structures and electrostatic fields on the sheet surfaces. A metastable rhombohedral phase of GaS was found to intergrow in this highly strained tubular structure. The present experimental observations suggest more complicated structure-dependent properties than theoretical predictions for the layered semiconducting compounds with tubular morphology.

Acknowledgment. F.-F.X. thanks the National Natural Science Foundation of China for financial support, and J.H. appreciates the Special Coordination Funds for Promoting Science and Technology from MEXT, Japan.

JA053340Z